NUCL SCI TECH (2017) 28:175
https://doi.org/10.1007/s41365-017-0327-3

Extraction chromatography–electrodeposition (EC–ED) process to recover palladium from high-level liquid waste

Qing Zou[1] · Shuai Gu[1] · Rui-Qin Liu[1] · Shun-Yan Ning[2] · Yan-Liang Chen[1] · Yue-Zhou Wei[1,2]

Received: 10 November 2016 / Revised: 17 April 2017 / Accepted: 29 April 2017 / Published online: 16 November 2017

Abstract The extraction chromatography–electrodeposition (EC–ED) process was proposed for the quantitative recovery of palladium from high-level liquid waste (HLLW) in this study. The process coupled the extraction chromatography method to obtain the decontamination of Pd(II) from HLLW with the electrochemical method to recover metallic palladium from the concentrated solution. Separation of Pd(II) from a nitric acid medium by extraction chromatography using *iso*Bu-BTP/SiO_2-P adsorbent and the electrochemical behavior of Pd(II) in nitric acid solution in the presence of thiourea (TU) were investigated. *iso*Bu-BTP/SiO_2-P exhibited a high selectivity for Pd(II) over other fission products (FPs), and Pd(II) could be desorbed by TU from loaded BTP/SiO_2-P. The adsorbent performed good stability against HNO_3 because the adsorption performance kept Pd(II) after extended contact with HNO_3 solution. The column experiment achieved the separation of Pd(II) from simulated HLLW successfully. The electrochemical behavior of Pd(II) in palladium desorption solution containing TU and nitric acid was investigated at a platinum electrode by cyclic voltammetry. A weak reduction wave at − 0.4 V was due to the reduction in Pd(II) to Pd(0), and the deposition process was irreversible. In electrowinning experiments, a maximum of 92% palladium could be obtained.

Keywords Palladium · HLLW · Extraction chromatography · Electrodeposition · BTP/SiO_2-P · Thiourea

1 Introduction

Palladium plays important roles in many industrial applications since it has unique and useful properties such as outstanding catalytic characteristics, good malleability, excellent electrical conductivity, and high chemical inertness [1]. There is an increasing demand for palladium. While its abundance in the earth crust is very low, spent nuclear fuel, as a valuable resource of noble metals, contains significant quantities of palladium. According to calculation, spent fuel contains about 1.3 kg Pd per ton from a light water reactor (LWR) at the burn-up of 33,000 MWd/t and about 11.1 kg Pd per ton from a fast breeder reactor (FBR) at the burn-up of 150,000 MWd/t [2]. Most of palladium in spent fuel would be transferred to high-level liquid waste (HLLW) generated from the PUREX process for the recovery of uranium and plutonium [3, 4]. Fission palladium is composed of stable isotopes, such as ^{104}Pd (17 wt%), ^{105}Pd (29 wt%), ^{106}Pd (21 wt%), ^{108}Pd (12 wt%), ^{110}Pd (4 wt%), and a radioactive ^{107}Pd (17% wt%) isotope, which is a soft β-emitter with a half-life of 6.5×10^6 a and a maximum energy of 35 keV [5]. On account of the intrinsic weak radioactivity of ^{107}Pd, almost all industrial equipments can tolerate the recovery process of radioactive palladium [6]. Furthermore, palladium would form separate phases during the vitrification

---

This work was supported by the National Natural Science Foundation of China (Nos. 11305102, 91126006, and 21261140335).

✉ Yue-Zhou Wei
yzwei@sjtu.edu.cn

[1] School of Nuclear Science and Engineering, Shanghai Jiao Tong University, Shanghai 200240, China

[2] Innovation Center for Metal Resources Utilization and Environment Protection, College of Resources and Metallurgy, Guangxi University, Nanning 530004, China

process of HLLW and cause deteriorations in the stability of the glasses [7]. So it is necessary to separate palladium from HLLW. Therefore, there is an increasing interest toward recovering palladium from HLLW.

So far, several separation methods were developed to recover palladium from HLLW, such as solvent extraction and sorption [8, 9], ion exchange [10], electrochemical approach [11–14], and extraction chromatography [15–17]. Among them, the electrochemical approach is a promising method owing to its advantages such as simplicity, cost effectiveness, and no need of additional reagents [14]. Koizumi et al. [11] achieved a recovery of 90% for the electrodeposition of Pd(II), and the electrodeposition rate increased with the rise in nitric acid concentration. However, because of the complexity of the HLLW, the recovery efficiency would be significantly lower due to other interfering competitive reactions. Jayakumar et al. [12] studied the electrochemical behavior of Pd(II) in simulated HLLW, and the recovery was below 40%. Kirshin et al. [13] reported the negative effects of HNO_3, $NaNO_3$, uranium, and other admixtures on the rate and the current efficiency of cathodic deposition of palladium. Thus, a combination method combining electrodeposition and other separation methods has become a trend and has received increasing attention [18, 19]. In the Advanced ORIENT Cycle proposed by Ozawa et al. [18], palladium recovery was achieved using a combination method consisting of ion exchange and electrochemical approach. Jayakumar et al. [19] developed a new extraction–electrodeposition (EX–EL) process to recover palladium, which achieved a good recovery.

Furthermore, our group has proposed an advanced partitioning process for trivalent minor actinides (MA (III)) separation from HLLW by the extraction chromatography method using BTP/SiO_2-P adsorbent [16]. According to our previous research results [17], *iso*hexyl-BTP/SiO_2-P exhibited extraordinarily high selectivity toward MA(III) and Pd(II). The adsorbed MA(III) can be eluted by water or diluted nitric acid solution, while Pd(II) cannot be eluted by water or nitric acid, but can be eluted efficiently by TU as eluting agent.

In this work, the selective adsorption of *iso*Bu-BTP/SiO_2-P toward Pd(II) and Pd(II) desorption behavior by TU from loaded BTP/SiO_2-P were researched. The stability of the adsorbent against nitric acid was investigated. Pd(II) separation by extraction chromatography using a column packed with *iso*Bu-BTP/SiO_2-P adsorbent was also conducted. Then, the electrochemical behavior of the Pd(II) desorption solution was investigated using cyclic voltammogram and electrodeposition. Based on these studies, the EC–ED process combining extraction chromatography using BTP/SiO_2-P adsorbent with electrodeposition from the eluent was proposed to recover palladium from HLLW. Thus, the EC–ED process is compatible with the MA separation process we have researched. TU as the eluting reagent could be the link between the extraction chromatography method and electrochemical approach as it is often be used as the eluent to desorb Pd(II) from a number of adsorbents [16, 17, 20–23].

2 Experimental

2.1 Materials

All the chemicals (including TU and nitrates of Pd(II), Ce(III), Sr(II), La(III), Dy(III), Eu(III), and Sm(III)) were of analytical grade. The extracting agent, *iso*Bu-BTP/SiO_2-P, was prepared as described in the previous study [24]. 0.5 g of *iso*Bu-BTP was impregnated into 1.0 g silica/polymer composite support (SiO_2-P). In other words, the content of the extracting agent was 33.3% of the total mass of the adsorbent. The SiO_2-P support with pore size of 0.6 µm, pore fraction of 0.69, and mean diameter of 50 µm contains a macroreticular styrene–divinylbenzene copolymer (SDB) which was immobilized in porous silica (SiO_2) particles (Shanghai Haiyuan Chemical Technology Co., Ltd., China). Figure 1a, b shows the chemical structure of *iso*Bu-BTP and SEM image of *iso*Bu-BTP/SiO_2-P, respectively.

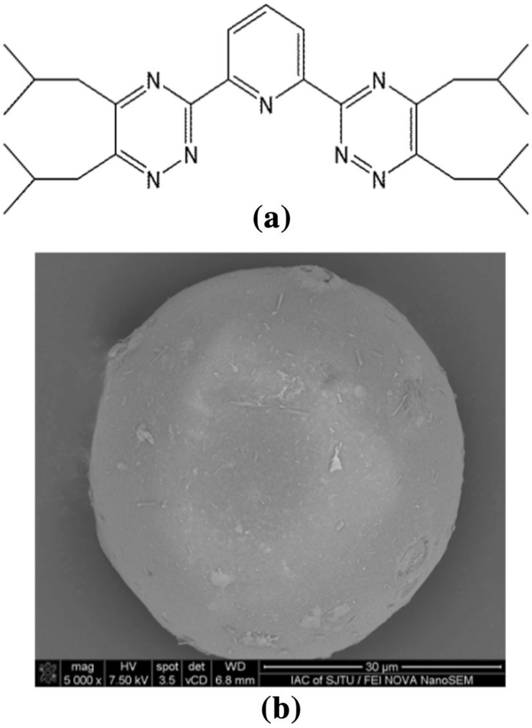

Fig. 1 Chemical structure of *iso*Bu-BTP (**a**) and SEM image of *iso*Bu-BTP/SiO_2-P (**b**)

2.2 Batch adsorption and batch desorption experiments

The adsorption of *iso*Bu-BTP/SiO_2-P adsorbent toward metal ions and the desorption of Pd(II) from loaded adsorbent were tested by batch experiments. In batch adsorption experiments, the solutions were prepared by dissolving metal nitrates into required concentration of nitric acid. For each batch experiment, 0.1 g adsorbent was combined with 5 mL aqueous solution in a glass vial with a screw cap. The mixture in the vial was shaken mechanically at 120 rpm at 298 K for a predetermined time in a water bath. The aqueous phase was filtrated through a membrane filter with 0.45 µm pore size. The concentrations of metal ions in solution were determined by an inductively coupled plasma atomic emission spectrometer (ICP-AES, Shimadzu ICP-7510, Japan).

The adsorption amount per unit adsorbent, Q (mmol g^{-1}), is calculated by Eq. (1):

$$Q = (C_0 - C_e) \times \frac{V}{W}, \tag{1}$$

where C_o and C_e (mmol L^{-1}) are the concentration of metal ions in the aqueous phase before and after adsorption, respectively; V(L) and W(g) indicate the volume of the aqueous phase and the weight of the dry adsorbent, respectively.

In batch desorption experiments, the loaded adsorbent was obtained by filtrating the adsorbent after 24 h of adsorption toward Pd(II). In consideration of the hydrolysis of Pd(II), the eluting solutions were made by dissolving TU in a low concentration of nitric acid. 0.1 g loaded adsorbent was contacted with 5 mL TU eluting solution and separated from the aqueous solution after 24 h. Then, the metal ion concentration was measured as described above.

The desorption performance was evaluated by using desorption efficiency, E (%), which was calculated by Eqs. (2) and (3).

$$Q_d = C_d \times \frac{V}{W}, \tag{2}$$

$$E = \frac{Q_d}{Q} \times 100\%, \tag{3}$$

where Q_d is the desorption amount in mmol g^{-1} and C_d indicates desorbed Pd(II) concentration in eluting solution in mmol L^{-1}.

2.3 Stability evaluation

To investigate the stability of the *iso*Bu-BTP/SiO2–P adsorbent against nitric acid, 0.1 g adsorbent and 5 mL nitric acid solutions were mixed into a glass vial, which was shaken mechanically at 120 rpm at a designed contact time. After filtrated and dried, the stability of the adsorbent was evaluated by batch adsorption experiments.

2.4 Column experiment

A glass column with a dimension of 5 mm in inner diameter and 500 mm in effective length packed with 4.3 g of *iso*Bu-BTP/SiO_2-P adsorbent was used for the column experiment. The column experiment was performed at 298 K by circulating the thermostated water through the water jacket of the column. The flow rate was controlled to 0.1 mL/min using a NPG-50UL Model pressure gage (Nihon Seimitsu Kagaku Co., Ltd., Japan) and a 2GN15K Model pressure limiter (Oriental Motor Co., Ltd., Japan). Before the experiment, a 15 mL HNO_3 (3 mol L^{-1}) solution was passed through the column to reach pre-equilibrium state. Then, the feed solution and different kinds of eluents subsequently flowed through the column. Effluents were collected every 15 min by an EYELA DC-1500 Model auto-fractional collector (Tokyo Rikakikai Co., Ltd., Japan). The concentrations of metal ions in the initial solution (C_0) and effluents (C) were determined by ICP-AES.

2.5 Cyclic voltammetry studies

The cyclic voltammetry of the desorption solution (10 mL) was recorded at a platinum plate ($\Phi = 2$ mm) working electrode at 298 K. The electrolyte was made by dissolving $Pd(NO_3)_2{\cdot}2H_2O$ into the appropriate concentration of nitric acid and TU in accordance with the desorption solution. A platinum plate (15 mm × 15 mm × 0.2 mm) was used as the counter electrode, and a KCl-saturated Ag/AgCl electrode (0.197 V vs. SHE) acted as reference electrode. Before each electrochemical experiment, the working electrode surface was polished with 1.0, 0.3, and 0.05 micro-gamma-alpha alumina powder in a sequence to a mirror finish and then washed in 3 mol L^{-1} HNO_3, acetone, ethanol, and distilled water in an ultrasonic cleaner for 10 min, respectively. At the same time, the solutions were deoxygenated by ventilating pure argon for 10 min. All the electrochemical experiments were controlled with an electrochemical workstation CorrTestTM model CS1350 equipped by electrochemical testing and analysis tool Version 4.3 software.

2.6 Electrodeposition studies

Electrolysis experiments were conducted on a titanium plate (50 mm × 50 mm × 2 mm) in desorption solution (100 mL). The electrolyte was made by dissolving $Pd(NO_3)_2{\cdot}2H_2O$ into 0.1 mol L^{-1} nitric acid and the appropriate concentration of TU. A platinum plate

(15 mm × 15 mm × 0.2 mm) and a KCl-saturated Ag/AgCl electrode (0.197 V vs. SHE) acted as the counter electrode and the reference electrode, respectively. After electrolysis, the electrolytes were examined by UV–VIS absorption spectrum and the concentrations of Pd(II) were determined by ICP-AES. The morphology and the composition of the electrodeposited palladium crystallizations were characterized by a low vacuum ultra-high-resolution field emission scanning electron microscope (LV UHR FE-SEM, OVA NanoSEM 230) with a large area silicon drift detector energy-dispersive spectrometer (Large Area SDD EDS, AZtec X-Max 80).

3 Results and discussion

3.1 Adsorption studies

Figure 2 shows the adsorption behavior of *iso*Bu-BTP/SiO_2-P toward the typical FPs contained in HLLW in different initial HNO_3 concentrations. As can be seen, Pd(II) showed a strong adsorption at all the examined HNO_3 concentrations. However, the adsorbent showed no or weak adsorption toward Ce(III), Zr(IV), Mo(VI), Sr(II), Ru(III), Nd(III), Y(III), and La(III). Dy(III), Eu(III), Sm(III), and Gd(III) exhibited a little stronger adsorption onto the adsorbent in ≥ 0.5 mol L^{-1} HNO_3 solution. So, the high selectivity of *iso*Bu-BTP/SiO_2-P toward Pd(II) is rather obvious. Pd(II) is a well-known soft metal ion, and the adsorption is considered to result from the complex formation with the soft ligand, *iso*Bu-BTP [16].

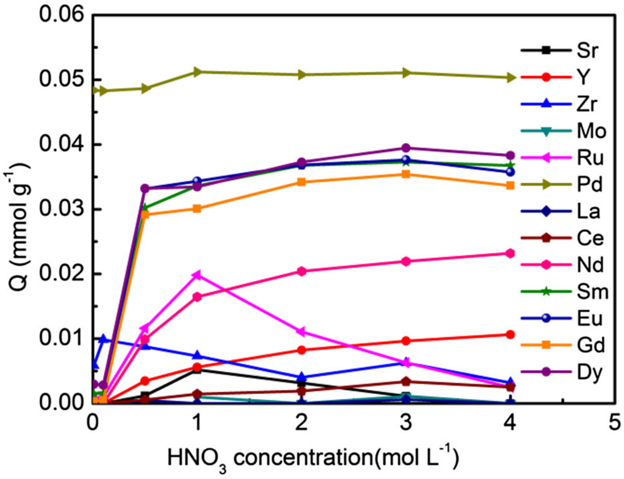

Fig. 2 (Color online) Effect of initial HNO_3 concentration on the adsorption capacity of some typical FPs in HLLW onto *iso*Bu-BTP/SiO_2-P adsorbent (metal ions, 1 mmol L^{-1}; adsorption conditions—phase ratio, 0.1 g/5 mL; temperature, 298 K; contact time, 24 h)

3.2 Desorption studies

The Pd(II) desorption efficiency from loaded *iso*Bu-BTP/SiO_2-P by TU is showed in Fig. 3. The effective elution of Pd(II) by TU from loaded BTP/SiO_2-P was achieved and was attributed to the fact that Pd(II) can form stable complexes with TU because of the soft atoms N and S contained in TU [22]. The desorption efficiency increased greatly by increasing the concentration of TU within 0.2 mol L^{-1}, and the desorption efficiency reached the maximum gradually. When the concentration of TU increased to 0.1 mol L^{-1}, 95% of palladium was desorbed. From Fig. 3, it can also be seen that the nitric acid concentration at 0.01 and 0.1 mol L^{-1} in eluting solution has little effect on the desorption efficiency. As the weak adsorption performance of the other FPs presented in Fig. 2 was under 0.01 mol L^{-1} HNO_3, 0.1 mol L^{-1} HNO_3 was chosen as the acid concentration of the TU eluent solution in the latter column experiment to avoid the possible elution of the other FPs by low acid concentration.

3.3 Stability evaluation

Due to the strong acidic environment of HLLW, the stability of the adsorbent was investigated by a set of experiments performed in 3 mol L^{-1} HNO_3. Figure 4 shows the effect of contact time with nitric acid solution on the adsorption of Pd(II) onto *iso*Bu-BTP/SiO_2-P. As can be seen, a small decrease in the adsorption amount of Pd(II) occurred after the contact with 3 mol L^{-1} HNO_3, and the adsorption showed almost no change as the contact time increased. The results indicate the adsorbent was affected

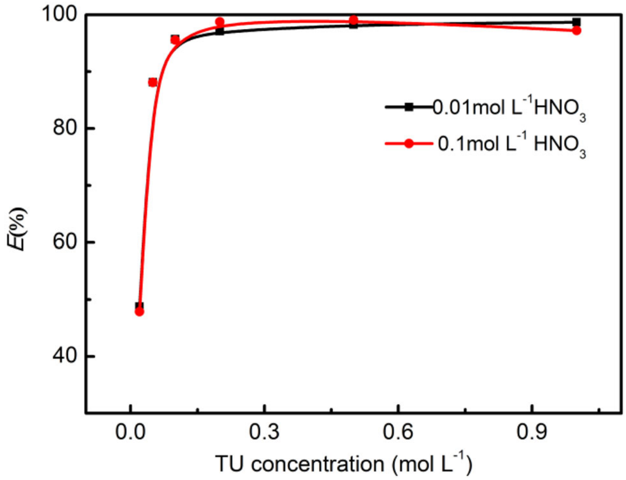

Fig. 3 (Color online) Effect of the concentration of TU on Pd(II) desorption from the loaded *iso*Bu-BTP/SiO_2-P adsorbent (adsorption conditions—phase ratio, 0.1 g/5 mL; temperature, 298 K; time, 24 h; [Pd], 10 mmol L^{-1}, 3 mol L^{-1} HNO_3; desorption conditions— phase ratio, 0.1 g/5 mL; temperature, 298 K; time, 24 h)

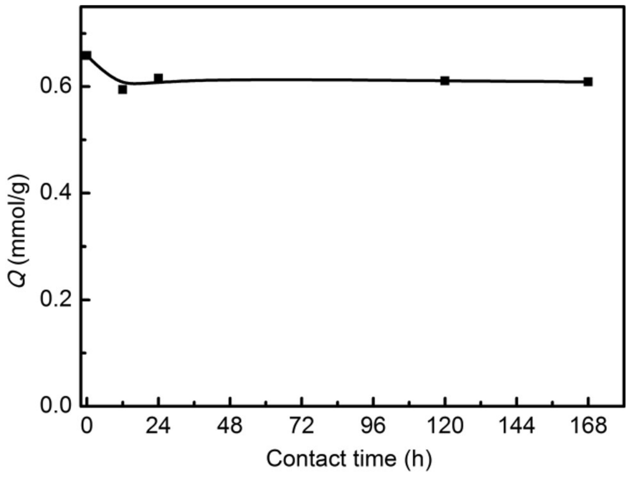

Fig. 4 Effect of contact time with nitric acid solution on the adsorption of Pd(II) onto *iso*Bu-BTP/SiO$_2$-P. (adsorption conditions— adsorbent: phase ratio: 0.1 g/5 mL; [Pd], 15 mmol L^{-1}; 3 mol L^{-1} HNO$_3$; temperature, 298 K; contact time, 24 h; shaking speed, 120 rpm)

by high concentrations of nitric acid and very limited quantities of extractant would be leaked into aqueous solution from the adsorbent. In consideration of the adsorption performance in long-time contact with 3 mol L^{-1} HNO$_3$ solution, *iso*Bu-BTP/SiO$_2$-P could be used a few more times in the column chromatographic process.

3.4 Column experiment

Based on the batch experimental results, the separation performance of Pd(II) from a 3 mol L^{-1} HNO$_3$ solution containing the typical FPs was conducted using the *iso*Bu-BTP/SiO$_2$-P adsorbent packed column. The concentration of metal ions in the feed solution was 1 mmol L^{-1}. After the feed solution passed through the column, the given volumes of 3 mol L^{-1} HNO$_3$, 0.1 mol L^{-1} HNO$_3$, and 0.1 mol L^{-1} HNO$_3$-0.1 mol L^{-1} TU were subsequently flowed through the adsorption column. The partitioning results are showed in Fig. 5.

As can be seen, La(III), Rh(III), Ru(III), and Ce(III) showed no or very weak adsorption and flowed through the column with the feed and washing solution. The other FPs, including Pd(II), were adsorbed strongly by the *iso*Bu-BTP/SiO$_2$-P adsorbent. These FPs, except Pd(II), were eluted by 0.1 mol L^{-1} HNO$_3$. Pd(II) was effectively eluted by using a TU solution. The elution band of Pd(II) is narrow and sharp, reflecting a fast elution dynamic. So, a successful separation of palladium from a nitric acid medium was achieved with a recovery ratio of more than 70%. These results indicate the feasibility to separate palladium from HLLW by extraction chromatography using BTP/SiO$_2$-P adsorbent. To recover metallic palladium, further electrochemistry studies were conducted toward palladium desorption solution, and the results were discussed below.

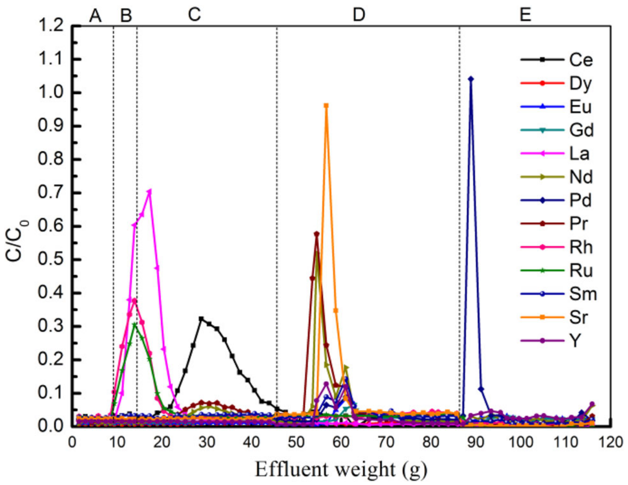

Fig. 5 (Color online) Results of Pd(II) separation from a simulated HLLW by an *iso*Bu-BTP/SiO$_2$-P adsorbent packed column (A: dead column, B: 5 mL feed solution, C: 30 mL 3 mol L^{-1} HNO$_3$, D: 40 mL 0.1 mol L^{-1} HNO$_3$, E: 30 mL 0.1 mol L^{-1} HNO$_3$-0.1 mol L^{-1} TU)

3.5 Cyclic voltammetry studies

Pd(II), nitrate ion, and TU tend to form complexes in an aqueous solution which would lead to a complex performance in the electrochemistry behavior of Pd(II). In order to understand the electrochemistry behavior of Pd(II), complexes formed in palladium desorption solution (10 mmol L^{-1} Pd(II), 0.1 mol L^{-1} TU, and 0.1 mol L^{-1} HNO$_3$) and their potentials are discussed first.

At 0.1 mol L^{-1} HNO$_3$, Pd (II) and a nitrate ion can mainly form one kind of complex [12], while Pd(II) and TU can form four kinds of complexes. Their formations in accordance with their stability constants are as follows [25]:

$$\mathrm{Pd}^{2+} + \mathrm{NO}_3^- \rightarrow \mathrm{Pd(NO_3)}^+, \quad \log\beta = 1.18, \tag{4}$$

$$\mathrm{Pd}^{2+} + \mathrm{TU} \rightarrow \mathrm{PdTU}^{2+}, \quad \log\beta_1 = 1.4, \tag{5}$$

$$\mathrm{Pd}^{2+} + 2\mathrm{TU} \rightarrow \mathrm{Pd(TU)}_2^{2+}, \quad \log\beta_2 = 3.1, \tag{6}$$

$$\mathrm{Pd}^{2+} + 3\mathrm{TU} \rightarrow \mathrm{Pd(TU)}_3^{2+}, \quad \log\beta_3 = 4.7, \tag{7}$$

$$\mathrm{Pd}^{2+} + 4\mathrm{TU} \rightarrow \mathrm{Pd(TU)}_4^{2+}, \quad \log\beta_4 = 8.3, \tag{8}$$

where β, β_1, β_2, β_3, β_4 are cumulative complex stability constants.

As the cumulative complex stability constants of Pd(NO$_3$)$^+$ are far less than Pd(TU)$_n^{2+}$, the complex of Pd(NO$_3$)$^+$ formed in the solution was so little that it can be negligible. In consideration of the total concentration of Pd^{2+} (10 mmol L^{-1}) and TU (100 mmol L^{-1}), the identical mass balance can be described using the following equations:

$$\left[Pd^{2+}\right]+\left[PdTU^{2+}\right]+\left[Pd(TU)_2^{2+}\right]+\left[Pd(TU)_3^{2+}\right]+\left[Pd(TU)_4^{2+}\right]=10, \tag{9}$$

$$[TU]+\left[PdTU^{2+}\right]+2\left[Pd(TU)_2^{2+}\right]+3\left[Pd(TU)_3^{2+}\right]+4\left[Pd(TU)_4^{2+}\right]=100, \tag{10}$$

After calculation, the results were (mmol L^{-1}): $[Pd^{2+}] = 3.867 \times 10^{-15}$ mmol L^{-1}, $[TU] = 60$ mmol L^{-1}, $[PdTU^{2+}] = 5.83 \times 10^{-12}$ mmol L^{-1}, $[Pd(TU)_2^{2+}] = 1.75 \times 10^{-8}$ mmol L^{-1}, $[Pd(TU)_3^{2+}] = 4.19 \times 10^{-5}$ mmol L^{-1}, and $[Pd(TU)_4^{2+}] \approx 10$ mmol L^{-1}.

The reduction process of palladium (II) can be described using Eqs. (11)–(13):

$$Pd^{2+}+nTU=Pd(TU)_n^{2+}\left(\Delta G_1^0=-RT\ln\beta_n\right), \tag{11}$$

$$Pd(TU)_n^{2+}+2e^-=Pd+nTU\ \left(\Delta G_2^0=-2FE_2^0\right), \tag{12}$$

$$Pd^{2+}+2e^-=Pd\left(\Delta G_3^0=-2FE_2^0\right), \tag{13}$$

The derivation of the value of reversible potential can be described as Eq. (14) [26]:

$$E_2^0=E_3^0-RT\ln\beta_n/2F, \tag{14}$$

where E_2^0 (*V*) is the reversible standard potential corresponding to each form of palladium complexes, $E_3^0 = 0.915$ V versus SHE; *R*, *T*, and *F* are the gas constant (8.314 J mol^{-1} K^{-1}), temperature (K), and Faraday constant (96,485 C mol^{-1}), respectively.

The reversible potential for each species (*E*) in the solution can be obtained by using the Nernst equation and considering the real concentration of each complex. The calculation results are given in Table 1. From the table, it is clear the dominant species in the desorption solution is $Pd(TU)_4^{2+}$ and its reduction happens at about − 0.019 V.

Then, the cyclic voltammogram of palladium desorption solution was recorded at a platinum plate electrode ($\Phi = 2$ mm) at a scan rate of 10 mV/s at 298 K, as shown in Fig. 6A. Three reduction peaks (a, b, and c) occurred continuously with small potential differences, which make it confused to figure out the Pd(II) reduction. To figure out the reaction that happened in the solution, the CVs of 10 mmol L^{-1} Pd(II) in 0.1 mol L^{-1} nitric acid (Fig. 6B) and 0.1 mol L^{-1} TU in 0.1 mol L^{-1} nitric acid (Fig. 6C) were obtained at the same scan rate and temperature.

Without the participation of TU, it is clear in Fig. 6B that the onset of Pd(II) reduction occurred at a potential of 0.4 V and the peak appeared at 0.27 V. At a more negative potential, the reduction peak at − 0.28 and − 0.4 V can be described as hydrogen adsorption on metallic palladium and hydrogen evolution reaction, respectively [14]. The oxidation peak occurred at − 0.18 V which suggests the desorption of hydrogen from palladium. Compared with Fig. 6B, the hydrogen adsorption and desorption disappeared in the addition of TU, as presented in Fig. 6A. It is obvious that the reduction potential of Pd(II) shifts much toward negative, while a small negative shift of hydrogen evolution (Fig. 6A(a)) is also observed.

TU would react on the electrode in a nitric acid solution, as shown in Fig. 6C. A wide electrochemical window is exhibited in Fig. 6C due to the adsorption of TU on the surface of the platinum electrode in the first scan cycle. When it comes to a positive potential, the adsorbed TU was oxidized and the electrode surface was exposed to the solution. Then, the Faradic current of TU series reduction occurred. As can be seen from Fig. 6C, the reduction potential of TU is very close to the calculated results of the Pd(II) reduction potential in Table 1. Therefore, TU would compete with Pd(II). In fact, TU has a very complex electrochemistry behavior in nitric acid solution. Equations (15–17) give the main reactions related to the redox of TU in nitric acid [27]. Compared with Fig. 6C, similar results were observed from Fig. 6A that TU would be adsorbed on the electrode and hinder the occurrence of the Faradic current of palladium and TU series reduction in the first scan cycle. Then, several current peaks were observed.

$$[Pt]\left((NH_2)_2CS\right)_{ad}\leftrightarrow\left[(NH_2)_2CS\cdot\right]^{+}+e, \tag{15}$$

Table 1 Potential of different kinds of complexes

Electroactive species	Concentration (mmol L^{-1})	E_2^0 (V)	*E* (V)
TU	60	–	–
Pd^{2+}	3.87×10^{-15}	0.718	0.203
$PdTU^{2+}$	5.83×10^{-12}	0.677	0.594
$Pd(TU)_2^{2+}$	1.75×10^{-8}	0.626	0.443
$Pd(TU)_3^{2+}$	4.19×10^{-5}	0.579	0.301
$Pd(TU)_4^{2+}$	10	0.472	− 0.019

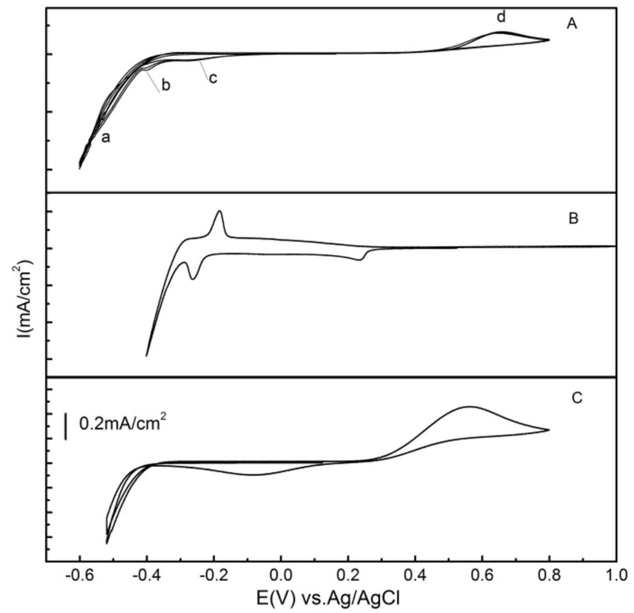

Fig. 6 Cyclic voltammograms of **a** 10 mmol L^{-1} Pd(II) in 0.1 mol L^{-1} nitric acid containing 0.1 mol L^{-1} TU, **b** 10 mmol L^{-1} Pd(II) in 0.1 mol L^{-1} nitric acid, and **c** 0.1 mol L^{-1} TU in 0.1 mol L^{-1} nitric acid

$$2\left[(NH_2)_2CS\cdot\right]^{+} \leftrightarrow \left[(NH_2)_2CSSC(NH_2)_2\right]^{2+}, \tag{16}$$

$$\left[(NH_2)_2CSSC(NH_2)_2\right]^{2+} \rightarrow S + NH_2CN + (NH_2)_2CS + 2H^{+} \tag{17}$$

After the above comparisons, the hydrogen evolution (Fig. 6A(a)), Pd(II) reduction (Fig. 6A(b)), and the redox of TU (Fig. 6A(c, d)) are cleared in Fig. 6A. The weak reduction wave at − 0.4 V suggests the deposition of Pd(II) and the deposition is typically an irreversible process. TU leads to a negative shift of Pd(II) reduction potential and can be comparative to the reduction in hydrogen and Pd(II). These results indicate that it is possible to recover palladium in metallic form by direct electrolysis from the desorption solution, and the results are discussed below. However, further research is still needed to reduce the negative impact brought by TU.

3.6 Electrodeposition studies of Pd

The working voltage was selected based on the cyclic voltammogram (Fig. 6). All the electrowinning studies were conducted on a titanium plate (50 mm × 50 mm × 2 mm).

The UV–Visible absorption spectrum of 0.1 mol L^{-1} TU and effect of electrolysis time on the UV–Visible absorption of the electrolyte at − 0.6 V were examined, and the results are shown in Fig. 7. There are two obvious absorption peaks located at 234 and 197 nm attributed to the characteristic absorption of TU. Compared with the UV–Visible absorption spectra of TU, the only absorption reduction in electrolytes performed at 234 nm indicates that Pd(II) forms complexes with the sulfur atom and the nitrogen atom has no interaction with Pd(II). It is clear that the complexes had a strong absorbance in the vicinity of 290 nm. With the increasing electrolysis time, the UV–Visible absorption of TU and palladium complexes both decrease, which indicates the deposition of palladium from palladium complexes accompanied by the consumption of TU on the electrode. The consumption of TU and palladium complexes was slow in the first hour and then became fast. After 6 h, the absorption of palladium complexes nearly disappeared, which indicates that most Pd(II) had been deposited.

The effect of electrodeposition time on the recovery ratio for the electrodeposition of Pd(II) (10 mmol L^{-1}) in 0.1 mol L^{-1} HNO_3 and 0.1 mol L^{-1} TU at three different potentials (− 0.5, − 0.6, − 0.7 V) is described in Fig. 8. As can be seen, the recovery ratio increased with increasing electrodeposition time at different potentials. After 6 h of electrolysis, recovery ratio of palladium at − 0.6 and − 0.7 V could reach 92%, higher than 85% at − 0.5 V. During the electrolysis, a small deposition rate of Pd(II) can be observed in the first hour due to the removal of TU from the electrode surface, which was consistent with UV–Visible absorption results. A higher deposition rate was accompanied by a higher working potential. However, the mean current efficiency for the electrodeposition of Pd at − 0.7, − 0.6, and − 0.5 V were 5.0, 7.6, and 11.0%, respectively. The interpretation for the low efficiency could be that the reduction in H^{+}, Pd(II), and TU happened at the

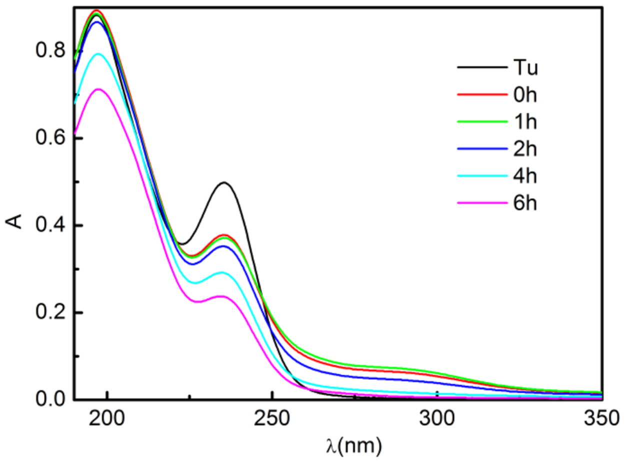

Fig. 7 (Color online) Effect of electrolysis time on the UV–VIS absorption spectrum of the electrolyte (initial solution: 10 mmol L^{-1} Pd(II), 0.1 mol L^{-1} HNO_3, and 0.1 mol L^{-1} TU), $T = 298$ K

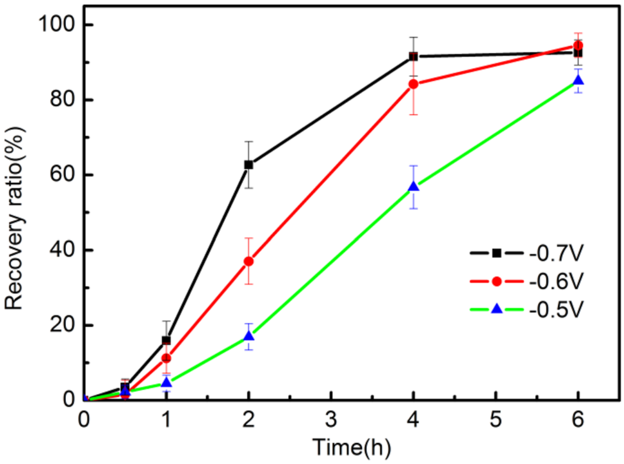

Fig. 8 (Color online) Effect of electrodeposition time on recovery ratio for the electrodeposition of Pd(II) from 0.1 mol L^{-1} HNO_3 and 0.1 mol L^{-1} TU at different working potentials at 298 K

same time due to their close reduction potential, which was consistent with the CV results.

Figure 9 shows the influence of TU concentration on the electrodeposition of Pd(II) (10 mmol L^{-1}) at a constant applied potential of − 0.6 V. It is clear that the curves obtained from three TU concentrations (0.05, 0.1, 0.2 M) are close to each other. All the recovery ratios that could reach about 90% after 6 h of electrolysis accompanied by and the mean current efficiency are 8, 7.6, and 6.5%, respectively. Lower current efficiency could be due to the competition of hydrogen evolution and the reduction in TU. The results indicate that TU makes a small difference to the recovery ratio in the range of this study concentration. However, TU greatly reduces the current efficiency due to the redox of TU series on electrodes. So the current efficiency of electrodeposition and rate of recovery of palladium can be improved and optimized by reducing or removing TU contained in the solution.

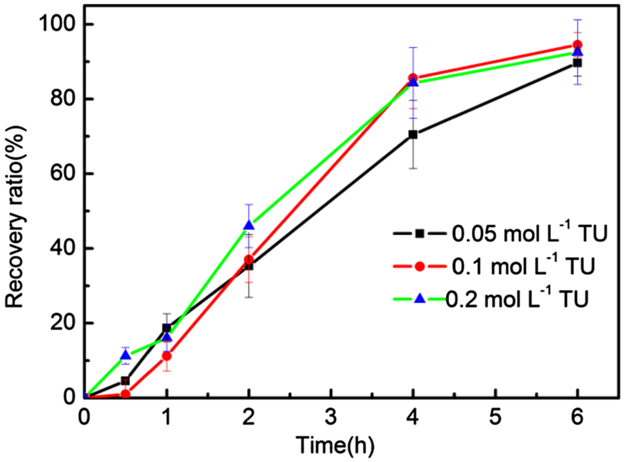

Fig. 9 (Color online) Recovery ratio for the electrodeposition of Pd(II) from different TU concentrations in 0.1 mol L^{-1} HNO_3 at − 0.6 V, $T = 298$ K

Figures 10 and 11 show the SEM and EDS characterization of palladium electrodeposition on the platinum electrode with $E = -0.6$ V for 30 min. From the SEM images (Fig. 10), a thick and relatively homogeneous and uniform distribution of palladium particles was observed. The clear dendrite morphology indicates a dendrite growth. In Fig. 11, the EDS pattern indicates that palladium was deposited successfully on the surface of the electrode. A small amount of sulfur would be deposited along with palladium during electrolysis, which would help palladium form a dense deposit [28]. The existence of sulfur could be removed by some technology, which still needs a further study.

3.7 Proposal of EC–ED process

The extraction chromatography method using the BTP/SiO_2-P adsorbent has shown a good performance in the separation of Pd(II) from nitric acid medium containing the typical FPs. Electrochemistry studies also verified the feasibility to recover palladium in metal form from desorption solution. According to these results, the conceptual flowchart of the EC–ED process for the recovery of palladium from HLLW was proposed, as shown in Fig. 12.

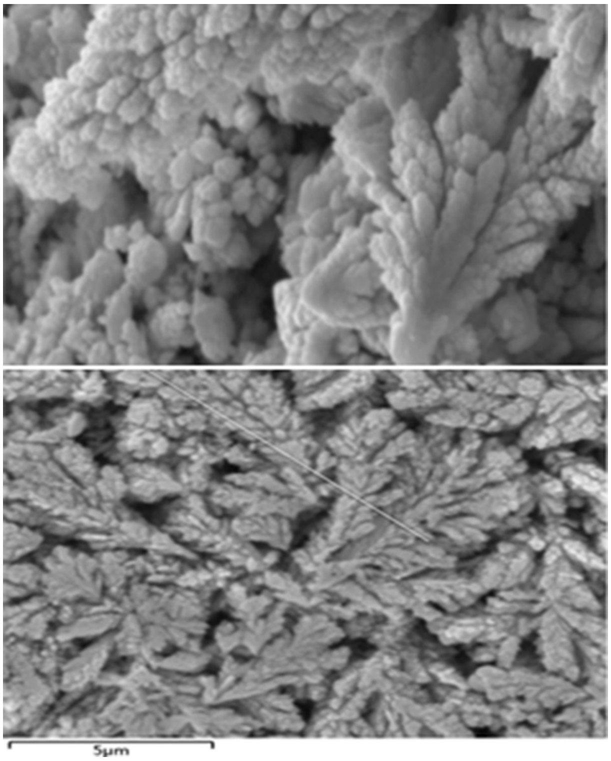

Fig. 10 SEM images of the palladium deposit obtained from 10 mmol L^{-1} Pd(II) in 0.1 mol L^{-1} nitric acid and 0.1 mol L^{-1} TU

Fig. 11 (Color online) EDS pattern of the palladium deposit obtained from 10 mmol L^{-1} Pd(II) in 0.1 mol L^{-1} nitric acid and 0.1 mol L^{-1} TU

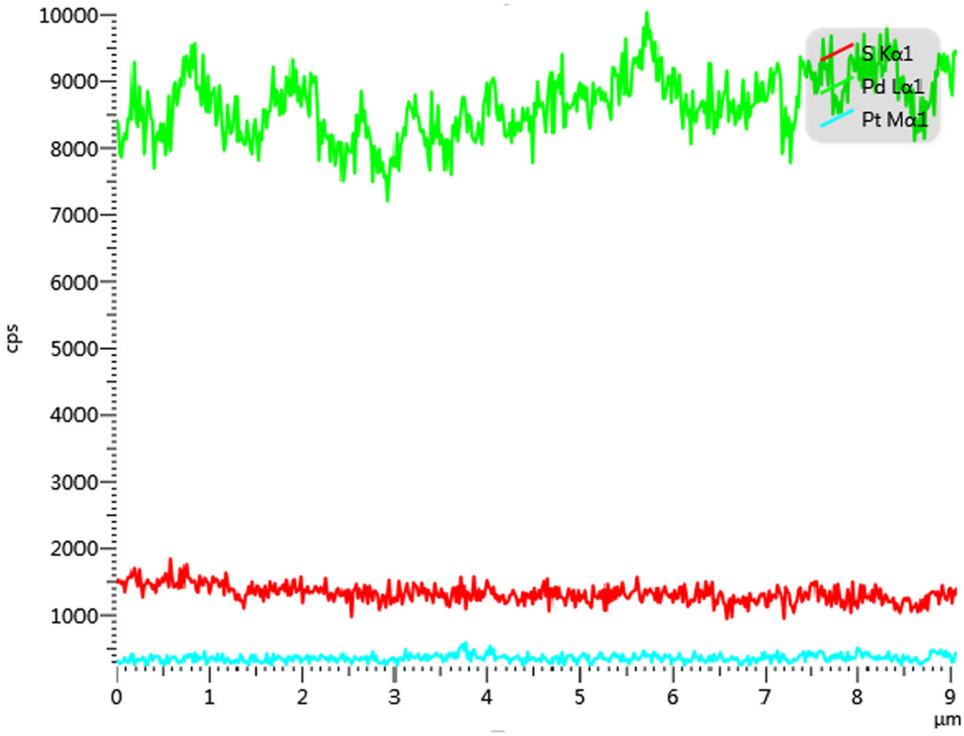

Fig. 12 (Color online) Conceptual flowchart of the EC–ED process for the recovery of palladium from HLLW

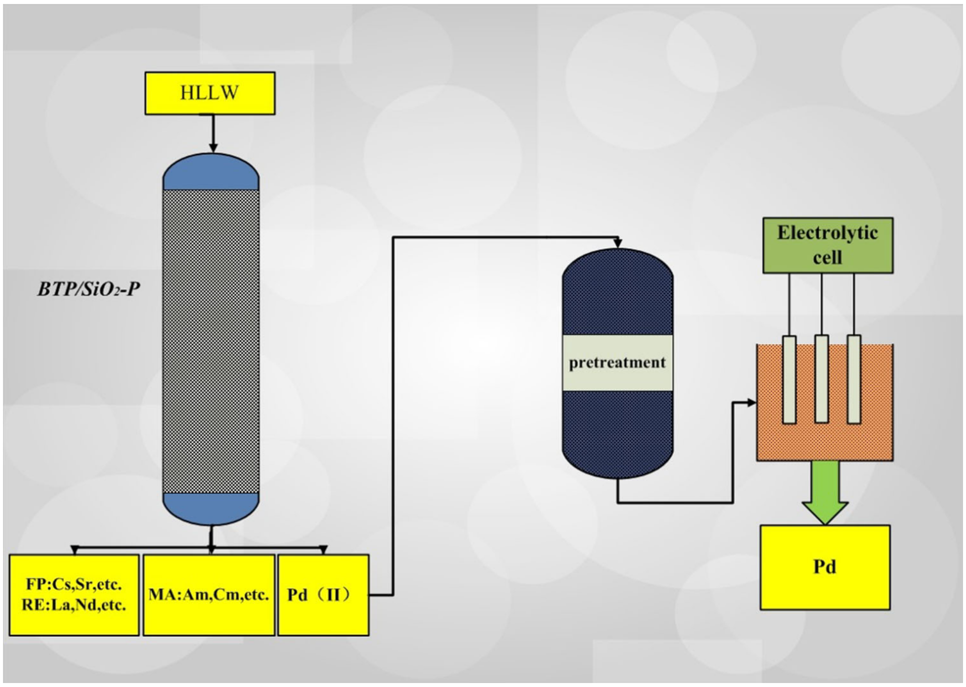

HLLW flowed through a column packed with BTP/SiO_2-P adsorbent. Pd(II) and MA could be effectively separated by choosing appropriate eluents. Then, the separated Pd(II) could be recovered by the electrodeposition method after some pretreatment. The eluent for the separation of palladium, such as TU, could be the link between the extraction chromatography method and electrochemical approach. Due to the complexity of HLLW, some host tests and optimum conditions still need to be studied.

4 Conclusion

The extraction chromatography–electrodeposition (EC–ED) process has been demonstrated for the recovery of palladium from nitric acid media. At all the examined HNO_3 concentrations, *iso*Bu-BTP/SiO_2-P performs a high selectivity and adsorption ability toward Pd(II). TU shows good palladium desorption performance from loaded *iso*Bu-BTP/SiO_2-P. 95% of palladium was desorbed at 0.1 mol L^{-1} TU. The adsorbent performed good stability against nitric acid. The column experiment achieves the separation of palladium from the nitric acid medium containing the typical FPs with a recovery of 70%. Pd(II) and TU could form four kinds of complexes in aqueous solution, which would lead to a negative shift of Pd(II) reduction potential. The cyclic voltammogram results show the reduction peak of palladium is located at − 0.4 V and the deposition process is irreversible. Palladium could be electrodeposited from the desorption solution, and the recovery ratio of Pd could reach 92%. The SEM–EDS characterizations of electrodeposited palladium indicate that the deposits perform a dendrite growth and the deposits are predominantly metallic palladium. Based on these results, the EC–ED process was proposed to recover palladium from HLLW. The process has the potential to be a kind of promising method for the recovery of Pd(II) from HLLW. Nevertheless, much more studies still need to be attempted to optimize the process.

References

1. G.M. Mudd, Sustainability reporting and the platinum group metals: a global mining industry leader? Platin. Met. Rev. **56**, 2–19 (2012). https://doi.org/10.1595/147106711X614713
2. K.A. Venkatesan, B.R. Selvan, M.P. Antony et al., Extraction of palladium from nitric acid medium by commercial resins with phosphinic acid, methylene thiol and isothiouronium moieties attached to polystyrene-divinylbenzene. J. Radioanal. Nucl. Chem. **266**, 431–440 (2008). https://doi.org/10.1007/s10967-005-0928-x
3. A. Dakshinamoorthy, P.S. Dhami, S.K. Munshi et al., Seperation of palladium from high level liquid waste, generated from reprocessing of PHWR spent fuel. BARC **292**, 7–16 (2008)
4. Y.A. Pokhitonov, V.N. Romanovskii, Palladium in irradiated fuel. Are there any prospects for recovery and application? Radiochemistry **47**, 3–14 (2005). https://doi.org/10.1007/s11137-005-0040-7
5. Z. Kolarik, E.V. Renard, Recovery of value fission platinoids from spent nuclear fuel. Platin. Met. Rev. **47**, 74–87 (2003)
6. S. Koyama, T. Suzuki, M. Ozawa, From waste to resource, nuclear rare metals as a dream of modern alchemists. Energy Convers. Manag. **51**, 1799–1805 (2010). https://doi.org/10.1016/j.enconman.2009.11.013
7. W. Grunewald, G. Roth, W. Tobie et al., The role of the platinum group elements ruthenium, rhodium and palladium in the vitrification of radioactive high level liquid waste using joule heated ceramic lined waste glass melters. Glass Technol Part A **6**, 266–278 (2008)
8. P. Giridhar, K.A. Venkatesan, T.G. Srinivasan et al., Extraction of fission palladium by Aliquat 336 and electrochemical studies on direct recovery from ionic liquid phase. Hydrometallurgy **81**, 30–39 (2006). https://doi.org/10.1016/j.hydromet.2005.10.001
9. D. Parajuli, K. Hirota, Recovery of palladium using chemically modified cedar wood powder. J. Colloid Interface Sci. **338**, 371–375 (2009). https://doi.org/10.1016/j.jcis.2009.06.043
10. S.H. Lee, H. Chung, Ion exchange characteristics of palladium and ruthenium from a simulated radioactive liquid waste. Sep. Sci. Technol. **38**, 3459–3472 (2003). https://doi.org/10.1081/SS-120023411
11. K. Koizumi, M. Ozawa, T. Kawata, Electrolytic extraction of platinum group metals from dissolver solution of purex process. J. Nucl. Sci. Technol. **30**, 1195–1197 (1993). https://doi.org/10.1080/18811248.1993.9734607
12. M. Jayakumar, K.A. Venkatesan, T.G. Srinivasan et al., Studies on the feasibility of electrochemical recovery of palladium from high-level liquid waste. Electrochim. Acta **54**, 1083–1088 (2009). https://doi.org/10.1016/j.electacta.2008.08.034
13. M.Y. Kirshin, Y.A. Pokhitonov, Recovery of Pd from spent fuel: 1. Electrochemical recovery of palladium from nitric acid solutions. Radiochemistry **47**, 365–369 (2005). https://doi.org/10.1007/s11137-005-0102-x
14. S. Liu, Y. Wei, R. Liu et al., Electrochemical behavior and electrowinning of palladium in nitric acid media. Sci. China Chem. **6**, 1743–1748 (2013). https://doi.org/10.1007/s11426-013-4945-2
15. A. Zhang, Y. Wei, T. Arai et al., Palladium removal from the simulated nuclear spent fuel solution using a silica-based SiPyR-N3 anion exchanger. Solvent Extr. Ion Exch. **24**, 447–462 (2006). https://doi.org/10.1080/07366290600646913
16. Y. Wei, X. Wang, R. Liu et al., An advanced partitioning process for key elements separation from high level liquid waste. Sci. China Chem. **55**, 1726–1731 (2012). https://doi.org/10.1007/s11426-012-4697-4
17. R. Liu, Y. Wei, Y. Xu et al., Evaluation study on properties of isohexyl-BTP/SiO_2-P resin for direct separation of trivalent minor actinides from HLLW. J. Radioanal. Nucl. Chem. **292**, 537–544 (2012). https://doi.org/10.1007/s10967-012-1631-3
18. M. Ozawa, S. Koyama, T. Suzuki, Nuclear rare metals and their separation in Advanced ORIENT Cycle strategy. Energy Procedia **7**, 421–424 (2011). https://doi.org/10.1016/j.egypro.2011.06.055
19. M. Jayakumar, K.A. Venkatesan, T.G. Srinivasan et al., Extraction–electrodeposition (EX–EL) process for the recovery of palladium from high-level liquid waste. J. Appl. Electrochem. **39**, 1955–1962 (2009). https://doi.org/10.1007/s10800-009-9905-3
20. S.Y. Kim, Y. Xu, T. Ito et al., A novel partitioning process for treatment of high level liquid waste using macroporous silica-based adsorbents. J. Radioanal. Nucl. Chem. **295**, 1043–1050 (2013). https://doi.org/10.1007/s10967-012-1878-8
21. R. Ruhela, J.N. Sharma, B.S. Tomar et al., N, N, N', N'-tetra(2-ethylhexyl) thiodiglycolamide T(2EH)TDGA: a novel ligand for the extraction of palladium from high level liquid waste (HLLW). Radiochim. Acta **98**, 209–214 (2010). https://doi.org/10.1524/ract.2010.1712
22. F. Bai, G. Ye, G. Chen, Highly selective recovery of palladium by a new silica-based adsorbent functionalized with macrocyclic ligand. Sep. Purif. Technol. **106**, 38–46 (2013). https://doi.org/10.1016/j.seppur.2012.12.021
23. Y. Xu, S.Y. Kim, T. Ito et al., Chromatographic separation of platinum group metalsfrom simulated high level liquid waste using macroporoussilica-based adsorbents. J. Chromatogr. A

1312, 37–41 (2013). https://doi.org/10.1016/j.chroma.2013.08.089

24. Y. Wei, M. Kumagai, Y. Takashima et al., Studies on the separation of minor actinides from high-level wastes by extraction chromatography using novel silica-based extraction resins. Nucl. Technol. **132**, 413–423 (2009)
25. Haynes WM (ed). *CRC Handbook of Chemistry and Physics*. CRC press, 2014
26. S. Gu, X. Wang, Y. Wei et al., Mechanism for nucleation and growth of electrochemical deposition of palladium(II) on a platinum electrode in hydrochloric acid solution. Sci. China Chem. **57**, 755–762 (2014). https://doi.org/10.1007/s11426-013-5026-2
27. J. Feng, Species analysis and kinetics study in the electrochemical oxidation of thiourea. Dissertation, China University of Mining and Technology, 2009 (**in Chinese**)
28. G.I. Lacconi, V.A. Macagno, Electrochemical study of thiourea in relation to the silver electrodeposition process. Electrochim. Acta **39**, 2605–2610 (1994). https://doi.org/10.1016/0013-4686(94)00229-0